

## Experimental studies of dynamic properties of Quaternary clayey soils



Wojciech Sas, Katarzyna Gabryś\*, Alojzy Szymański

Faculty of Civil and Environmental Engineering, Warsaw University of Life Sciences – SGGW, Warsaw, Poland

### ARTICLE INFO

#### Keywords:

Dynamic properties  
Cohesive soils  
Shear modulus at small strains  
Secant shear modulus  
Resonant column test

### ABSTRACT

The recent significant development of technical infrastructures in Poland, along with the construction of tower blocks, roads, railways and underground rapid transit system, resulted in greater demands for investment projects as well as geotechnical data characterizing the variation of various soil parameters found in the subsoil. The most important parameter, which represents the stiffness of soil deposits, is the shear modulus  $G$ . Therefore, this study focused on determining the initial shear modulus of cohesive soils from the area of the capital of Poland. In this research, a set of the resonant column (RC) tests was performed and the influence of three selected factors, i.e. mean effective stress ( $p'$ ), void ratio ( $e$ ) and plasticity index ( $PI$ ), on the low-amplitude shear modulus ( $G_0$ ) was presented and discussed. The results obtained from laboratory tests indicated that the stress state plays an important role for the small-strain shear modulus values of the Polish Quaternary cohesive soils. In contrast, there was no clear trend observed for the significant effect of  $e$  or  $PI$  on  $G_0$  for the studied soils. Based on the performed tests, the authors proposed the power-law relations for  $G_0$  versus  $p'$  of the forms:  $G_0 = 3.02p'^{0.68}$  and  $G_0 = 0.82p'^{0.96}$ .

### 1. Introduction

Over sixty years, a significant amount of research has been carried out in order to understand better the mechanical response of soils under dynamic excitations. A variety of laboratory techniques were used for these studies, e.g. cyclic torsional shear tests, cyclic direct simple shear tests, cyclic triaxial tests and resonant column tests. They allowed researchers to define the impact of many factors, most importantly of strain amplitude and frequency of excitation, on soil behaviour (Lai et al. [1]).

In 1937, two Japanese engineers, Ishimoto and Iida, developed the first resonant column test method [2]. Then, in the 1960's this equipment was popularised by such scientists as Hall and Richart in 1963 [3], Drnevich, Hall and Richart in 1967 [4] as well as Hardin and Black in 1968 [5]. In the last 40 years, some improvements and modifications of the design of the first resonant column testing device were made. Drnevich helped to standardize the whole test procedure and developed more complicated mathematical models to be used in these tests (Drnevich [6]).

For proper seismic response analysis, as well as for the development of soil modelling programme, an appropriate investigation of dynamic soils properties is essential (Rayhani and El-Naggar [7]). When describing the soil dynamic characteristic, the most important are two following characteristics: the dynamic shear modulus and the damping ratio (Senetakis et al. [8]). These parameters are required in

order to build the Hardin-Drnevich [9] model, which describes the stress-strain relationship (Nie et al. [10]).

To investigate dynamic properties of soils, the resonant column test is applied. The basic principle of this kind of test is to vibrate a cylindrical soil sample in an elemental mode of vibration: torsion or flexure. Historically, it has been used to estimate the small-strain shear modulus  $G_{max}$  (frequently designated as  $G_0$ ), the small-strain material damping  $D_{min}$  as well as the relationship between the shear modulus  $G$ , the material damping  $D$  and the shear strain  $\gamma$  in soils and soft rocks (Kalinski and Thummaluru [11], Yang and Yan [12]). The resonant column tests are performed in order to understand better the mechanisms affecting stiffness (Schneider et al. [13]).

According to the ASTM Standard (ASTM [14]), the vibration of the sample may be superposed on a controlled ambient state of stress in the specimen. The vibration apparatus and specimen are typically enclosed in a triaxial chamber and subject to an all-around pressure and an axial load. Additionally, the specimen may be subject to other controlled conditions, such as: pore-water pressure, degree of saturation or temperature. These test methods of the shear modulus and damping determination are considered non-destructive when the strain amplitudes of vibration are less than  $10^{-4}$  rad ( $10^{-4}$  in./in.). Under such conditions, many measurements can be carried out on the same specimen and under various states of the ambient stress.

The series of experiments and analyses herein were performed to study dynamic properties of normally consolidated soils from Warsaw,

\* Correspondence to: Water Centre – Laboratory, Warsaw University of Life Sciences – SGGW, 6 Ciszewskiego Street, 02-776 Warsaw, Poland.  
E-mail address: [katarzyna\\_gabrys@sggw.pl](mailto:katarzyna_gabrys@sggw.pl) (K. Gabryś).



Fig. 1. Photography of GDS Resonant Column Apparatus with tested sample.

based on the GDS Resonant Column Apparatus (RCA). An experimental study was performed, using a modern laboratory device, in order to investigate the small- to medium-strain soil behaviour. In this article, the test equipment and the research programme, as well as the results obtained, are presented and discussed next.

## 2. Experimental setup

The GDS Resonant Column Apparatus is used in this study (Fig. 1) to excite one end of a isotopically confined solid cylindrical soil specimen. This apparatus is an example of fixed–free resonant column (Sas and Gabryś [15]). In this system, an upright cylindrical specimen of soil, with an aspect ratio of 2:1 (length: diameter), is employed (Kalinski and Thummalur [11]). The ratio of the length over the diameter amounts typically to: 100×50 mm or 140×70 mm. The soil specimen is usually fixed at the base (*passive end*), but is free at the top (*active end*) to oscillate in torsion or in flexure (a precise description of torsional and flexural test can be found in e.g. Cascante and Santamarina [16]). The instrumentation, placed on the top of the sample, includes a loading cap, an electromagnetic drive system incorporating precision wound coils and a permanent magnet, a counter-balance and an accelerometer. Energisation mode of coils is switchable by software in order to provide the torsional and bending tests (longitudinal).

The GDS Resonant Column Apparatus includes a very strong connection between coils and the support plate. Each pair of coils are encased in a Perspex jacket, which is rigidly connected to the support plate. A magnetically neutral, circular plate is connected to the top of each Perspex block to fit all the coils together. Additionally, the support cylinder is designed in a manner, which ensures a maximum rigidity. The GDS Apparatus also minimizes the damping effect of the equipment. The software can switch the hardware to provide an ‘open circuit’ during free vibration decay, which prevents from a back electromotive force generation (Cascante et al. [17]).

The GDS device is equipped with a standard cell, capable of achieving 1 MPa gaseous cell pressure. Back pressure is applied by the GDS Standard pressure/volume controller. The specimen is placed in a latex membrane and it is tested in a pressurized cell. To reinforce the membrane sealing, the system is equipped with an inner cell for silicon oil (Cascante et al. [17]). The axial deformations of the sample

are measured with an internal LVDT, which is mounted inside the confining chamber (Khan et al. [18]).

The resonant column test is an effective method of determining  $G_O$ ,  $\xi_O$ , and  $G$ ,  $\xi$  as a function of  $\gamma$ , where  $G$  is the dynamic shear modulus,  $\xi$  is the damping ratio and  $\gamma$  is the shear strain. There are some general rules in determining above-cited parameters. The column specimen is prepared and then consolidated. The frequency of the electromagnetic drive system is slowly increased, until the first mode resonant condition is encountered. The value of the resonant frequency is known, which allows the back-calculation of the wave propagation velocity ( $V_s$  –S-wave velocity) and thereby establishing  $G_O$  (taking into account the sample geometry and the conditions of end restraint). After measuring the resonant conditions, the electromagnetic drive system is cut off and the column specimen is brought to a state of free vibration.  $\xi_O$  is calculated by observing the decay pattern (Cascante et al. [17]).

## 3. Tested soils

For their laboratory tests, the authors chose samples in the vast majority with medium fines content,  $10\% < FC < 20\%$ . The selected moraine clayey soils are commonly found in Poland, also in a large part of the Warsaw area, where, nowadays, more and more engineering challenges emerge, such as: underground constructions or development of new railways and roads. Therefore, using the European classification [19], the laboratory experiments were conducted on clayey sands (clSa), silty clays (siCl), sandy clays (saCl) and sandy silty clays (sasiCl). The range of the index properties of the investigated soils is presented in Table 1. Their specific gravity was equal to  $2.71\text{g/cm}^3$ .

The position of the soils in the plasticity chart is shown in Fig. 2. According to the plasticity chart, all samples were identified as average cohesive and cohesive soils (CL). The authors in their research were tested semi-solid,  $LI < 0$ , and hard-plastic soils,  $0 < LI < 0.25$ , with a various level of plasticity, from slightly plastic,  $3\% < PI < 15\%$ , to medium plastic soils,  $15\% < PI < 30\%$ .

The first test site was located on one section of the expressway No. S2, between its two nodes: “Konotopa” and “Airport”, in the area of the road embankment No. WD-18 (Fig. 3). The road embankment No. WD-18 is one of the twenty embankments on the Southern Warsaw Bypass S2, along its nodes: “Konotopa”-“Airport” (PIG [20]). The soil in this area was investigated to a depth of 25.0 m and there can be found the complex of cohesive soils - plastic and stiff clays with interbeds of sand.

The second test site was situated in the region of Pelczyńskiego Street, in Bemowo, one of the western districts of Warsaw (Fig. 3). In this area, under the surface of turf and uncontrolled embankments, a layer of dammed lake materials was located, e.g. cohesion-less (fine sands, silty and loamy sands) and below them existed cohesive dammed soils (clays, compacted clays and silts, with distinct bands of fine and silty sands). Dammed materials were found mostly up to the depth of about 4.0–5.0 m. Then, a layer of moraine soils (sandy clays and clayey sands) was located, until the maximum depth of about 10.0–13.0 m. Next, grey river sands were found, reaching the depth of 15.0 m.

A standard routine sampling procedure was employed in order to guarantee the consistency of the samples. One of the sampling methods, for the most samples, was a collection of the samples in block forms. Thereby, the sampling process was very cautious, so as not to affect the structure of the soil. The second way of sampling was by collecting the drilled material in the Shelby type, cylindrical probes, but only for test site No. 2. The samples for laboratory tests were collected right below at the ground surface (at the depth around 0.5 m) and next, from shallow depths of approx. 2.0 and 2.5 m. The block samples, for example, were carefully trimmed at the depth of 2.0 m from an excavated pit. All collected samples were sealed and stored in a humidity room until needed.

The material represented one geological layer for each test site. In

**Table 1**  
Physical properties of the selected soil specimens.

Soil type	Soil name	Depth m	$\rho^a$ g/cm <sup>3</sup>	$W^b$ %	$LL^c$ %	$PL^d$ %	$PI^e$ %	$LI^f$ –	$p^g$ kPa	$e_0^h$ –
clSa	S2-1	0.5	1.93	14.0	33.5	14.5	19.0	–0.03	10–30	0.60
siCl	S2-2	0.5	2.08	12.0	37.6	13.9	23.7	–0.08	10–30	0.46
sasiCl	S2-3	2.0	2.23	10.2	30.8	11.9	18.9	–0.09	45–180	0.34
clSa	S2-4	2.0	2.23	12.8	31.2	12.6	18.6	0.01	45–315	0.37
clSa	S2-5	2.0	2.20	12.2	31.0	12.0	19.1	0.01	45–225	0.38
clSa	S2-6	2.0	2.12	13.3	31.5	12.7	18.8	0.03	45–315	0.45
saCl	S2-7	2.0	2.17	12.2	37.0	11.5	25.6	0.03	45–315	0.40
clSa	S2-8	2.0	2.16	15.6	41.7	14.3	27.5	0.05	45–315	0.45
clSa	S2-9	2.0	2.16	14.4	36.8	12.7	18.8	0.03	45–315	0.46
clSa	S2-10	2.0	2.16	14.2	35.2	11.4	23.8	0.12	45–315	0.43
sasiCl	B-1	2.5	2.19	13.6	27.8	12.8	15.2	0.05	55–165	0.40
sasiCl	B-2	2.5	2.17	12.7	27.1	12.3	14.8	0.01	55–165	0.40
sasiCl	B-3	2.5	2.15	12.2	37.0	11.5	25.6	0.03	55–165	0.42

<sup>a</sup>  $\rho$ =bulk density.  
<sup>b</sup>  $W$ =initial water content.  
<sup>c</sup>  $LL$ =liquid limit.  
<sup>d</sup>  $PL$ =plasticity limit.  
<sup>e</sup>  $PI$ =plasticity index  $PI=LL-PL$ .  
<sup>f</sup>  $LI$ =liquidity index  $LI=(W-PL)/(LL-PL)$ .  
<sup>g</sup>  $p'$ =mean effective stress  $p'=(\sigma'_1+2\sigma'_3)/3$ .  
<sup>h</sup>  $e_0$ =initial void ratio.

the case of both, block and tube samples, for laboratory experiments, the samples located next to each other in the field were investigated. Therefore, there was no difference in the samples quality. The block samples were obtained, in particularly, in order to have relatively identical samples from the same horizon. They could be used to verify the effects of various parameters on the dynamic soil properties. Additionally, some tube samples were also tested since they were used mainly to compare the soil dynamic properties between two types of samples. In the case of the samples from test site No. 1, they were characterized as normally consolidated ( $OCR=1$ ), while the material from test site No. 2 was classified as lightly overconsolidated ( $OCR=1.2$ ). Then, in laboratory, the soil e.g. from cylindrical probes was carefully pulled out and, from the least damaged fragments of the probes, using a special mould, the right size specimens were cut out.

**4. Test programme**

The adopted test programme can be found as well in other articles of the authors (e.g. Sas and Gabryś [15], Sas et al., 2012 [21]), which relate to the same topic. In this paper, though, they would like to present the most important stages of their experiments, detailing some

of the applied novelties.

Only cylindrical samples with intact structure were investigated, each one with a diameter of approx. 7.0 cm and height of approx. 14.0 cm. The implementation of the resonant column test consisted of several phases. Before the proper dynamic measurements were performed, the soil required correct preparation. The sample installation procedure and the initial stages of the study, namely modelling the natural conditions of samples in field, are the same as in the case of conventional triaxial test.

The initial stages of the measurements included: flushing of the equipment (especially saturation of the pore pressure system), specimen's saturation, control of Skempton's parameter  $B$  and consolidation. These procedures are identical to that used in conventional triaxial testing. There are, however, two important differences. To speed up the consolidation process and to compensate the faster dissipation rate of pore water pressure, filters made from paper strips were attached around the entire side surface of the sample. Moreover, to reduce the diffusion of air through a latex membrane, in which the sample is equipped, two membranes were used and a layer of silicone was placed between them during the early tests. In later studies, only one membrane remained, but a special tube (so-called “inner cham-

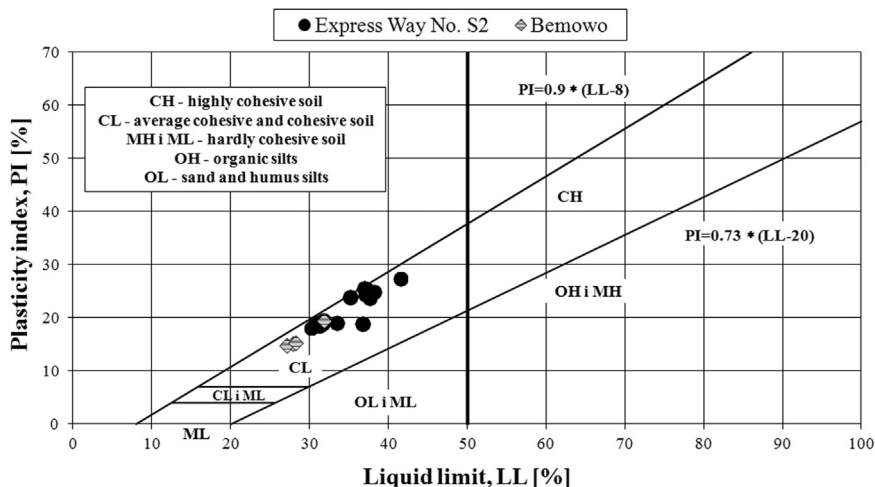


**Fig. 2.** Plasticity chart of tested soils.

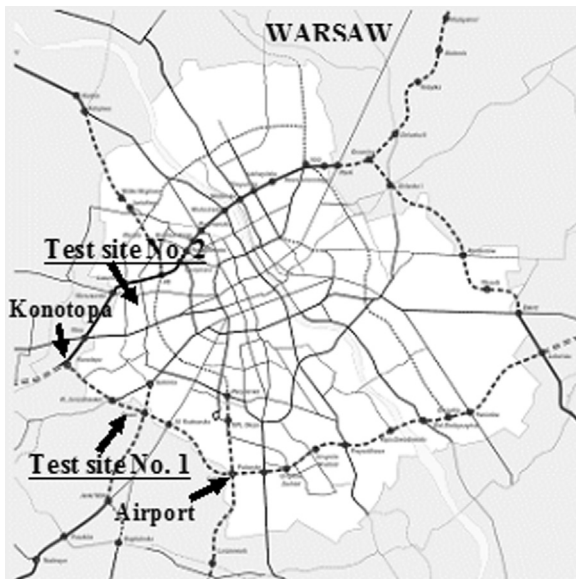


Fig. 3. Localization of tested sites: test site No. 1 – Expressway No. S2, test site No. 2 – Pelczyńskiego Street in Warsaw.

ber”) filled with distilled water was applied and placed in the test material.

Undisturbed material was set up in the cell, and then saturated by the back pressure method. During this stage, a small amount of cell and back pressures were applied in steps, with a consequent dissolution of the air contained in the intergranular spaces. The pressures were increased slowly, to ensure proper saturation of the specimen until the Skempton's  $B$  value was higher than 0.9 (Skempton [22]). The values of the applied pressures were determined depending on the effective stress at this stage of the study and taking into account the conditions of the swelling phenomena. In order to prevent the process of swelling, the employed effective stress was always higher than the swelling pressure for each analysed sample. When full saturation was achieved, the isotropic consolidation process started.

Consolidation was initiated by opening the drainage valves connecting the specimen to the volume change device. The specimen was subjected to the same back pressure used during the last saturation step while the cell pressure was various, dependent on the mean effective stress  $p'$  required in the next steps. The values of the effective isotropic stress level were changed, adopting the rule that the first consolidation is carried out by  $p'$  equal to in-situ stress level (e.g.  $\sigma'_{v0}=45.0$  and  $55.0$  kPa, adequately for the material from test site No. 1 and No. 2). The level of the mean effective pressure during the next consolidation had the appropriate higher value, e.g.  $2\sigma'_{v0}=90.0$  kPa,  $3\sigma'_{v0}=135.0$  kPa,  $4\sigma'_{v0}=180.0$  kPa, etc. (see Table 1 for details of  $p'$  for each specimen). The limitations of the apparatus resulted in the maximum achieved effective stress reaching the level of approx. 315 kPa during consolidation process in the GDS Apparatus. Sometimes, due to technical reasons, the maximum effective stress was not achieved (e.g. specimens S2-3, S2-5, B-1, B-2, B-3). Special attention should be paid to the first two specimens (S2-1 and S2-2), for which the range of the mean effective stresses is different. It was related to their shallow location and also some technical difficulties.

During the consolidation phase, the volume change and the axial deformation of the specimen were measured. Moreover, the void ratio of the sample was updated during consolidation at each loading stage. For all the tests, the consolidation process itself lasted at least until the end of the initial consolidation phase, usually around 24 h (or sometimes 48) (Flores-Guzmán at el. [23]), using additional strips of filter paper, as mentioned before. At this point, prior to the dynamic tests, the readings and baselines were taken of various monitoring equipment. The resonant column tests were performed in undrained

conditions.

In order to excite the electromagnetic field and induce a wave propagating through the examined material, the corresponding coil voltage values were placed. The magnetic field in the coils interacted with the magnets attached to the driving plate, that in turn conveyed a torsional oscillation to the top of the specimen. In this research, the authors started with the coil voltage value of 0.1 V and performed tests with voltage increasing in 0.1 V increments up to a final value of 1.0 V. As the frequency of the input signal varied, the dynamic response of the specimens resulted in a varying motion amplitude. The amplitude was captured by an accelerometer. The frequency maximizing the motion of the specimen's top was associated to the first-mode resonance and was found by applying an input signal with a frequency sweep. The secant shear modulus of the tested material was evaluated from the resonant frequency.

At a given mean effective stress value, the RC tests were repeated several times, increasing progressively the amplitude of the input voltage, thus obtaining the shear modulus corresponding to increasing values of the shear strain (Amir-Faryar and Aggour [24]).

## 5. Obtained results and their interpretation

### 5.1. Effect of various factors on dynamic properties of the analysed soils

In this part of the article, the authors presented the most important results of their laboratory tests. They studied the influence of such factors as void ratio, effective stress level and plasticity index on the tested soils' stiffness. Particularly, they checked the possible variation of the shear modulus with the strain amplitude (Markowska-Lech at el. [25]).

At small strains ( $\gamma < 10^{-5}$ ), the phenomenon of stress-strain loop reduction occurs, and it is adopted to an almost straight line. After Vucetic [26] and Lombardi at el.[27], there exists a strain level, the threshold linear shear strain  $\gamma_{te}$ , for which no stiffness degradation is observed. An elastic behaviour of soil appears with no permanent microstructural changes of its fabric with dynamic loading. The secant shear modulus  $G$  decreases, as the strain amplitude increases beyond  $\gamma_{te}$ . The soils behaves non-linearly. It is common to indicate the effect of strain on  $G$  very often by the ratio  $G/G_0$  (so-called the normalized shear modulus). Hence, some example stiffness reduction curves of the analysed consolidated soils in saturated conditions are shown in Fig. 4. In this figure, typical experimental data obtained from the resonant column tests for the specimens from test site No. 1 (specimens S2-4, S2-6, S2-7, S2-8, S2-9, S2-10) are plotted. Moreover, the stress dependency is noticeable here as well. On the basis of this figure the following can be observed: firstly,  $G/G_0$  ratio decreases with the rise of the strain amplitude and, secondly, in most cases the higher effective stress, the less significant the reduction of  $G/G_0$  ratio at the same strain level. This tendency has not been confirmed, however, for two mean effective stresses, 45 and 90kPa. For example, the modulus ratios for  $p'=45$ kPa give the uppermost data points. This was probably due to some limitations of the device itself, as well as some troubles to find the resonant frequency at small strains and small pressures.

The authors carried out a set of the RC tests on isotropically consolidated cohesive soils under various values of the effective stress  $p'$ . Although the RC test is a reliable and accurate method for measuring the low-amplitude shear modulus  $G_0$  (Cai at el. [28]), some of its characteristics should be borne in mind. The RC test is possible namely in the relatively small strain range. A number of loading cycles prior to measurement is unknown, the authors expect it to be approximately thousands of cycles. Additionally, the loading frequency is high, reaching the order of 100 Hz and more. Fig. 4 indicates exactly this small strain scope between  $10^{-4}\%$  and  $10^{-1}\%$ , while Fig. 5, on the other hand, illustrates the variation of  $G_0$  with the effective stress. Both use the logarithmic scale for the all analysed specimens. In Fig. 4, a

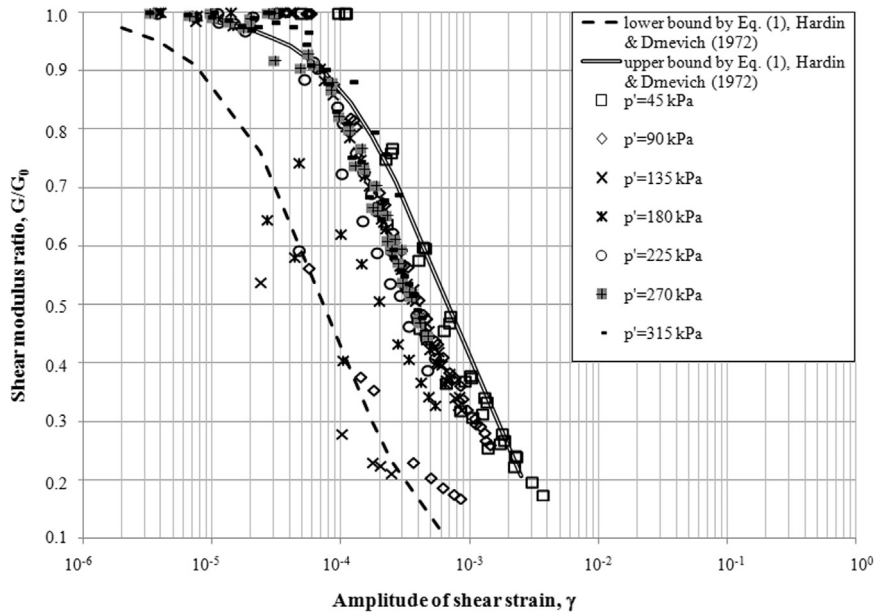


Fig. 4. Experimental normalized shear modulus curves versus shear strain for Polish Quaternary clayey soils.

scatter of results is visible, which may be due to previously mentioned constraints as well as the slightly different clayey soil samples investigated. Furthermore, the upper and lower bounds of degradation curves are proposed. The authors used the equation suggested by Hardin and Drnevich [9] for undisturbed cohesive soils in order to determine the normalized shear modulus and the bounds. The equation is given as follows

$$\frac{G}{G_0} = \frac{1}{1 + \frac{\gamma}{\gamma_r}} \tag{1}$$

where  $\gamma_r$  is the reference shear strain. As proposed e.g. by Stokoe et al. [29], the reference strain corresponds to the shear strain amplitude when  $G/G_0$  ratio is equal to 0.5. In order to calculate the bound lines, the diverge results (data points for  $p'=45$  and  $90$  kPa) are rejected, the results for  $p'=135$  and  $315$  kPa are used instead. The reference shear

strain amounts therefore approx.  $7.5 \cdot 10^{-5}$  for  $p'=135$  kPa and  $6.5 \cdot 10^{-4}$  for  $p'=315$  kPa. It can be seen that most of the experimental data generated from the present work fall within the band defined by Hardin and Drnevich [9].

In Fig. 5a linear or quasi linear increase of  $G_0$  with  $p'$  on a log-log plot is shown. In fact, it means that the modulus exhibits a power-law dependence on effective stress, as is well-known from many previous studies in the literature such as Hardin and Drnevich [9]. The influence of the mean principal effective stress is admittedly assumed as one of the two very important factors; so is void ratio, which remarkably affects the low-amplitude shear modulus of clayey soils (Hardin et al. [4], Wichtmann et al. [30]). It is noticeable here as well, that the results for soil specimens S2-1 and S2-2 stand out in comparison with other results. These two specimens were actually test samples obtained from shallow depths and, therefore, were studied at lower effective stresses

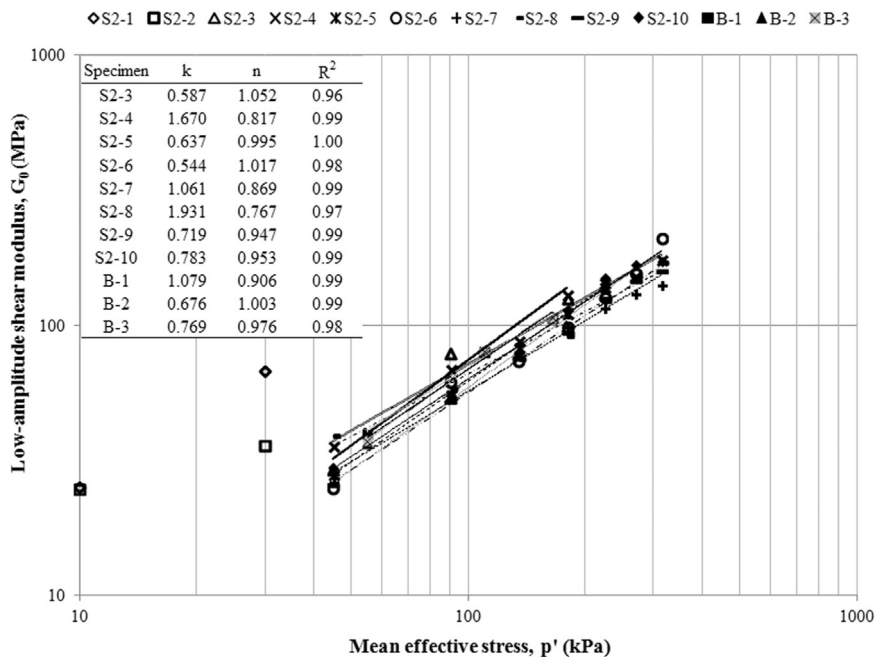


Fig. 5. Low-amplitude shear modulus of Polish Quaternary clayey soils as functions of mean effective stress.

than the rest of the specimens. The authors also aimed to examine the dynamic properties of the soils found at shallow depths, which are suitable for shallow foundations.

The influence of the mean effective stress on  $G_0$  can be assessed as well from the best-fitting parameters of the power regression curves presented in Fig. 5. The generic function of these curves, which relates  $G_0$  (in MPa) to  $p'$  (in kPa), is given in Eq. (2).

$$G_0 = k(p')^n \quad (2)$$

The parameters  $k$  and  $n$  are the best-fit power regression constants. According to the literature (e.g. Pineda et al. [31]), the constant  $k$  can be associated with the values of  $G_0$  at  $p'=1$  kPa and reflected directly the influence of the soil's original microstructure. The second constant  $n$ , on the other hand, can be related to the slope of the power regression curve and represented the susceptibility of the soil skeleton to changes in  $p'$ .

The values of the power regression constants together with the coefficients of determination  $R^2$  are summarized in Fig. 5 as well. For S2-1 and S2-2 specimens the curve fitting was not done due to the low number of data points. Constant  $k$  values range from 0.544 to 1.931, the variation of this constant is very low. Values of  $n$  range between 0.767 and 1.052, the differences of the pressure exponent  $n$  are slight too. Calculated values confirm that tested specimens behave identically and, in the most analysed cases, the variation of the low-amplitude shear modulus with effective pressure follows well the linear relation on double logarithmic graph. It should be noted, though, that  $n$  values in this research are greater than reported for example by Hardin and Drnevich [9]. It can be indicated that Quaternary clayey soils from Warsaw area are more susceptible to the application of  $p'$  in terms of  $G_0$  and become stiffer with changes in pressure, faster than another soils studied in the literature.

In Fig. 6 the effect of void ratio  $e$  on  $G_0$  of the selected cohesive soils from Warsaw area is presented. General trend from Fig. 6 show that the increase of the shear modulus with the decrease of void ratio. This observation is consistent with the previous results found in the literature, e.g. Hardin and Black [5]. From the analysis of the plotted results, it can be assumed that the changes of void ratio for each sample during the RC tests are very small, around 1.6%. The small variations in  $e$  values among all tested specimens may be due to sampling from one depth and testing finally the uniform specimens. In this case, it is difficult to reach great differences in void ratio. Therefore, it seems necessary to consider the appropriateness of using this parameter to create the model for determining  $G_0$  regarding the block clayey

samples from Warsaw. The outstanding specimen was specimen S2-6, characterized by the greatest values of low-amplitude shear modulus, over 210 MPa. For this specimen, consequently, the curve  $G_0=f(e)$  reached the highest position.

Similarly to the study of  $p'$  effect on the shear modulus, in the case of void ratio the nonlinear dependence of  $G_0$  on  $e$  given by Eq. (3) is proposed as well.

$$G_0 = k \frac{1}{e^n} \quad (3)$$

The form of the equation is derived based on the well-known formula from Hardin and Drnevich [9]. In Fig. 6 additionally, the summary of the power regression constants ( $k$ ,  $n$ ) and the coefficients of determination  $R^2$  is included, except specimens S2-1, S2-2 and S2-3. Although the values of  $R^2$  are high, which show a very good adaptation of this model to the experimental data, the best-fit power regression constants seem to be considerably higher than those determined in the literature. The small variation of the void ratio during the RC tests on one sample may confirmed the former observation about the study of quite stiff material.

In the previous publication on normally consolidated and moderately overconsolidated clays (Dobry and Vucetic [32]), it was concluded that the plasticity index correlates well with significant parameters, as well as with some aspects of dynamic behaviour such as the small-strain shear modulus. Dobry and Vucetic [33] found that for normally consolidated soils ( $OCR=1$ )  $G_0$  does not depend on the plasticity of the soil, while for overconsolidated soils ( $OCR > 1$ )  $G_0$  increases with plasticity. The possible effect of plasticity on dynamic behaviour of the tested clayey soils appears in Fig. 7. It should be outlined here that all tested specimens had  $PI$  smaller than 30%, as summarized in Table 1.

In Fig. 7a, the values of  $G_0$  versus plasticity index for the specimens from test site No. 1 are shown. The authors analysed the results from the RC tests at three selected stresses, namely 135, 225 and 315 kPa. The examined specimens are characterized by different  $PI$  values, range from 18.6 to 27.5. As shown in Fig. 7a, there is no trend relating  $PI$  with the low-amplitude shear modulus for the examined normally consolidated clayey soils from test site No. 1. Hence, the independence of the relation between  $G_0$  from  $PI$ , noticed and experimentally verified by researchers including e.g. Hardin and Black [5] or Hardin [34], is observed in this study as well.

The authors studied the effect of plasticity index on  $G_0$  for overconsolidated soils on the basis of the experimental data from test site

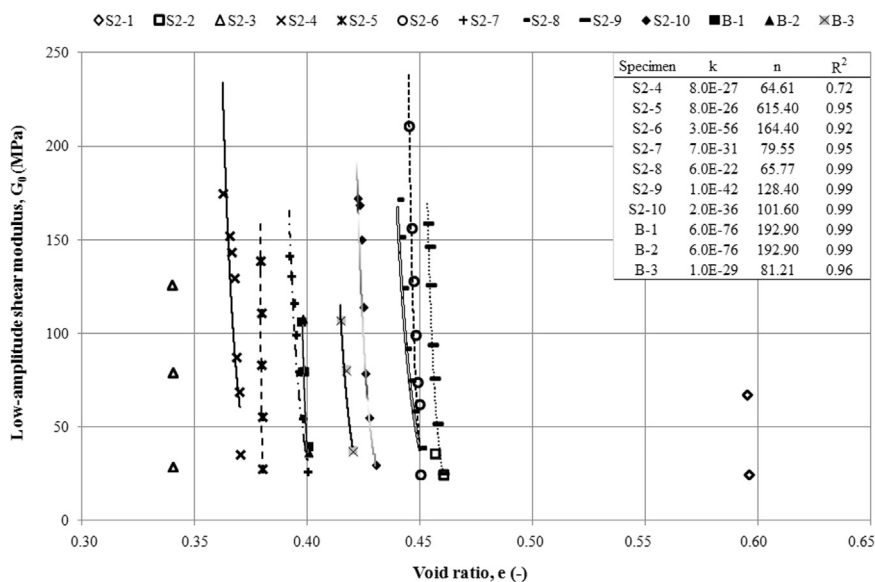


Fig. 6. Low-amplitude shear modulus of Polish Quaternary clayey soils as functions of void ratio.

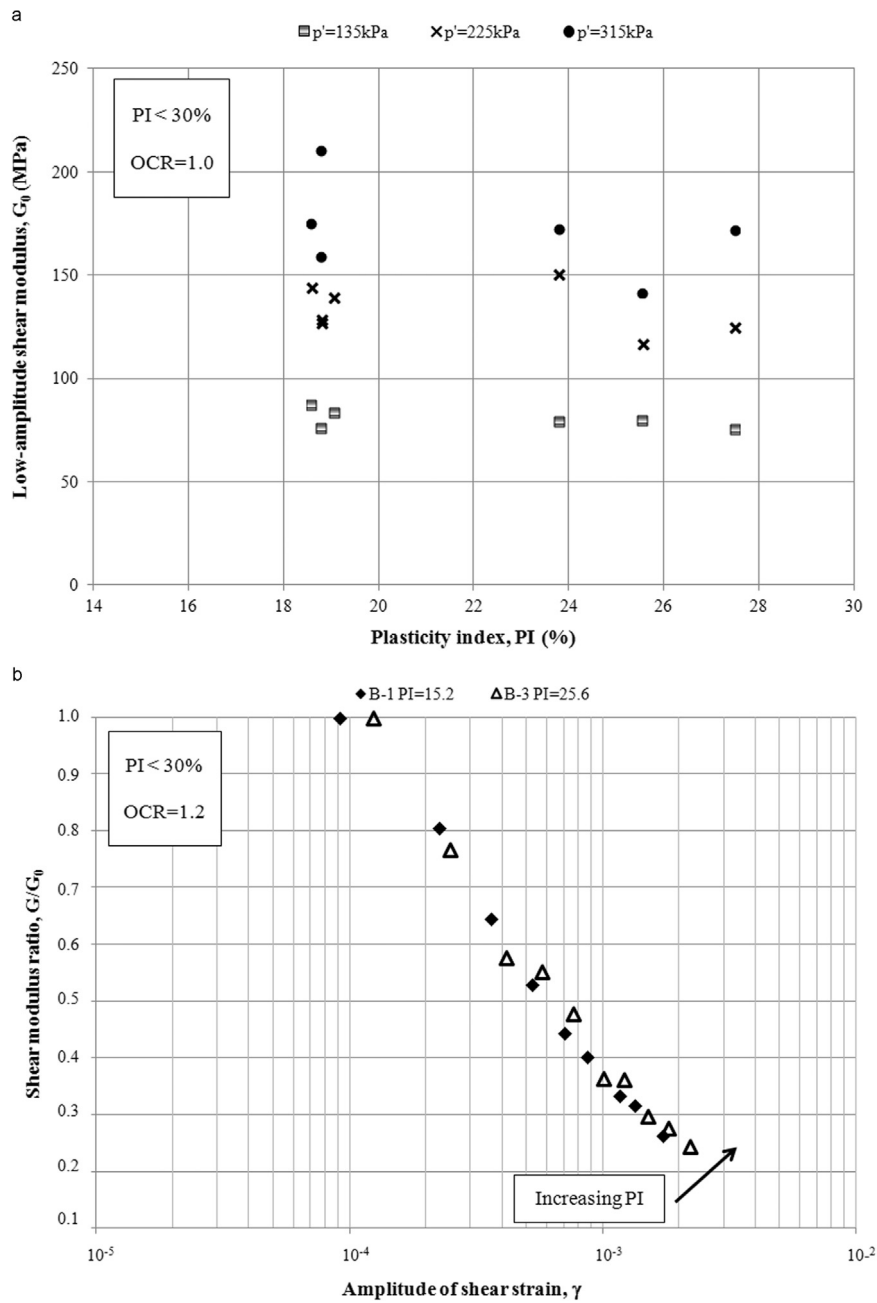


Fig. 7. Relations between  $G$  and  $G/G_0$  versus  $\gamma$  and soil plasticity for normally (a) and slightly overconsolidated (b) Polish Quaternary clayey soils.

No. 2 (Fig. 7b). In this figure, the trend between  $PI$  and the  $G/G_0$  curves for slightly overconsolidated soils is analysed. The  $G/G_0$  curves versus  $\gamma$  tend to move up as  $PI$  increases. Similar observations were reported by Dobry and Vucetic [32] or Kokusho et al. [35].

It would be worthy to obtain similar measurements from more cohesive soils. The greater  $PI$  is associated with more linear elastic behaviour, which may imply less discrete nature of soil.

### 5.2. The statistical reliability of the results

One of the necessary tools for assuring the quality assurance of the work are the statistical operations. They are necessary to control, as well as to verify, the analytical procedures and the resulting data. Therefore, in this subsection of the article, some basic statistical treatment of data will be considered.

In Table 2 basic statistics for the low-amplitude shear modulus  $G_0$

are summarized. The mean effective stress is an independent variable. Using the programme STATISTICA (version 10.0) the following parameters were defined: mean, confidence interval and median, as well as e.g. variance and standard deviation with confidence interval for standard error. In order to verify the reliability of the laboratory test results and their possible future use for the analysis of soil deformation in the range of small and medium strains, the authors estimated the uncertainty of measurements and calculations. It is worth noticing that standard error of the mean value of  $G_0$  for all of the presented data is rather low, not exceeding the value of 10 MPa. This confirms the regularity of the conducted research. For samples from test site No. 1, it is clear that together with the change in the stress level the standard error rises to the highest value for the maximum value of analysed effective stress. In the case of standard deviation distribution of  $G_0$  the results are similar. The lowest variance between the soil stiffness values refers to the lowest level of stress. For example, in case of soil from test

**Table 2**  
Descriptive statistic for the low-amplitude shear modulus at each mean effective stress.

	Test site No. 1							Test site No. 2		
	Mean effective stress, kPa							Mean effective stress, kPa		
	45	90	135	180	230	270	315	55	110	165
<b>Shear modulus, <math>G_0</math></b>										
Average	31.5	58.0	79.7	106.2	132.4	150.3	164.2	38.0	80.8	107.3
Confidence -95%	24.1	49.2	73.7	86.4	114.9	133.5	146.8	33.7	78.9	105.4
Confidence +95%	38.8	66.2	85.7	126.0	149.9	167.1	181.5	42.2	82.6	109.1
Median	30.0	55.5	79.2	99.7	126.6	152.1	172.1	37.4	80.8	107.3
Minimum	25.8	52.4	75.4	92.1	116.7	131.0	141.7	36.6	80.0	106.5
Maximum	39.3	69.0	87.6	130.0	150.3	168.8	175.2	39.9	81.5	108.0
Interval	13.5	16.6	12.2	37.9	33.6	37.8	33.5	3.3	1.5	1.5
Variation	35.0	42.7	23.2	254.2	198.2	183.3	195.0	3.0	0.6	0.6
Standard Deviation	5.9	6.5	4.8	15.9	14.08	13.5	14.0	1.7	0.8	0.8
Confidence Intervals Std. Dev. -95%	3.6	3.9	2.9	9.6	8.4	8.1	8.4	0.9	0.4	0.4
Confidence Intervals Std. Dev. +95%	17.0	18.8	13.8	45.8	40.5	38.9	40.1	10.8	4.7	4.7
Standard Error	2.7	2.9	2.2	7.1	6.3	6.1	6.2	1.0	0.4	0.4

site No. 2, the values of standard error and standard deviation for  $p'=110$  and  $165\text{kPa}$  are exactly the same. Slightly higher values were obtained for the lowest stress.

Additionally, the authors conducted an errors analysis compiled in Table 3. Three types of errors were counted and presented in this table. When comparing the values of the all estimated errors, it can be observed that they are low, which shows high accuracy and correctness of the parameters recorded during the laboratory tests.

5.3. Experimental model describing the soil deformation characteristics in the range of small strains

One of the aims of the following research was to identify the factors that influence the dynamic properties of the selected Quaternary clayey soils from Warsaw area. These properties are represented here by the low-amplitude shear modulus  $G_0$ . In order to investigate the relationship between  $G_0$  and chosen factors, described in the subsection 5.1. of this article, the correlation analysis was carried out. This analysis, using the correlation model, allows for the evaluation of the expected value of a random variable on the basis of a single representation of another random variable that is correlated with the first variable. It is important that the correlation has the cause and effect character. The main indicator of the strength of the relationship between two measurable variables is the Pearson correlation coefficient, or shortly the correlation coefficient  $R$ . The correlation coefficient shows the strength and the direction of the relationship between variables. Its values depend on the interval  $[-1; 1]$ . If the resulting value is closer to zero, it means that this relationship is weaker;  $R$  values closer to 1 (or  $-1$ ) result in a stronger relationship. A value of 1 indicates a perfect linear relationship (it is often obtained in the course of correlation analysis of random features A with feature A).

In Table 4 the correlation matrix for the tested specimens from both

test sites and the values of the Pearson correlation coefficient are shown. On the basis of the conducted analysis, it was found that the mean effective stress  $p'$  has the largest impact on the initial stiffness  $G_0$  of all tested soils ( $R=0.96$  – test site No. 1 and  $R=0.99$  – test site No. 2)  $R$  values close to unity reflect very strong correlation between  $G_0$  and  $p'$ . For the other analysed factors, i.e. void ratio  $e$  and plasticity index  $PI$ , only weak correlation was ascertained, otherwise there was no correlation. This may be indicated by the low values of  $R$  regarding  $e$  and  $PI$ . A different tendency should be expected, especially because the extensive world-wide laboratory and field studies have already clarified many aspects of the influence of mean effective confining stress, stress history, soil type, plasticity index and soil microstructure on the dynamic response of soil materials (Dobry and Vucetic [33]). However, with respect to the selected Quaternary clayey soils from Warsaw area, the authors substantially limited the number of elements to one (i.e.  $p'$ ) needed for further calculation. Two others parameters were considered statistically insignificant.

In order to select a suitable equation describing the soil deformation characteristics in the range of small strains, the regression analysis was performed. As a result of this analysis, the following empirical formulas are proposed (separately for both test sites):

$$G_0 = 3.02 \cdot p'^{0.68} \tag{4}$$

$$G_0 = 0.82 \cdot p'^{0.96} \tag{5}$$

where Eq. (4) stands for test site No. 1 and Eq. (5) for test site No. 2.

Subsequently, a comparison of the results from the present work with those previously reported for cohesive soils was conducted. The authors examined few well-known and widely used  $G_0$  relations to verify their possible prediction of the low-amplitude shear modulus of Polish Quaternary clayey soils. The following equations were selected, suggested by:

**Table 3**  
The estimated errors of the  $G_0$  measurements at each mean effective stress.

	Test site No. 1								Test site No. 2			
	Mean effective stress, kPa								Mean effective stress, kPa			
	45	90	135	180	230	270	315	Average	55	110	165	Average
Average absolute error, MPa	-1.5	-3.4	-2.1	-3.8	1.6	4.1	-0.7	-0.8	-1.3	0.4	0.4	-0.2
Average relative error, %	0.01	-0.05	-0.02	-0.02	0.02	0.03	0.01	0.002	-0.03	0.01	0.004	-0.01
Corrected average relative error, MPa	32.9	61.4	81.8	110.0	130.8	148.6	162.5	104.0	39.4	84.1	109.4	77.5

**Table 4**  
Correlation matrix – test site No. 1 and No. 2.

Test site No. 1						Test site No. 2							
	Average	Standard deviation	$G_0$	$p'$	$e$	$PI$		Average	Standard deviation	$G_0$	$p'$	$e$	$PI$
$G_0$	100.3	50.0	1.00	<b>0.96</b>	0.13	-0.08	$G_0$	75.3	30.3	1.00	<b>0.99</b>	-0.15	0
$p'$	167.8	94.6	<b>0.97</b>	1.00	0.21	0.01	$p'$	110.0	47.6	<b>0.99</b>	1.00	-0.14	0.0
$e$	0.43	0.06	0.13	0.21	1.00	<b>0.41</b>	$e$	0.40	0.01	-0.15	-0.15	1.00	<b>0.98</b>
$PI$	22.0	3.5	-0.08	0.01	<b>0.41</b>	1.00	$PI$	18.5	5.3	0	0	<b>0.98</b>	1.00
	$p'$	$e$	$PI$					$p'$	$e$	$PI$			
$G_0$	<b>0.96</b>	0.13	-0.08				$G_0$	<b>0.99</b>	-0.15	0			

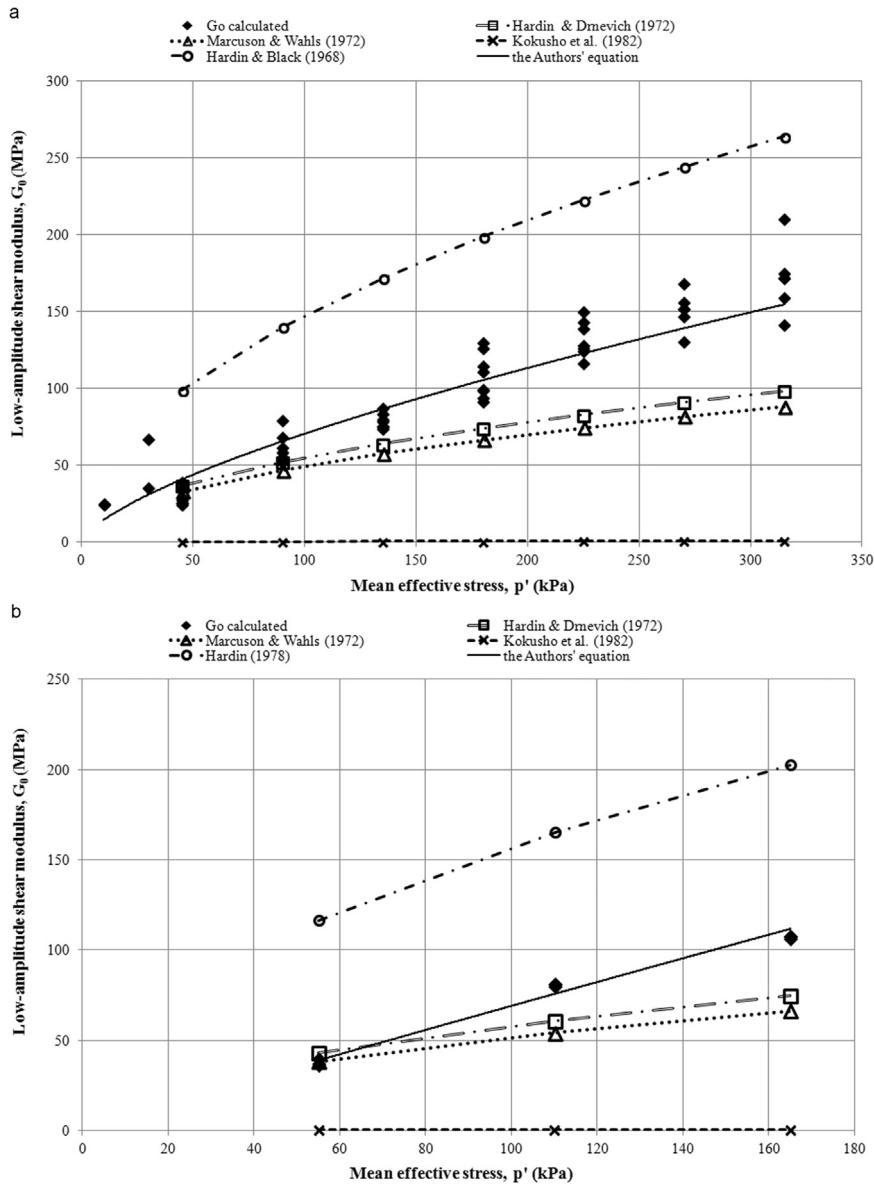


**Fig. 8.** Comparison of the fitting capacity of the authors' equations and standard empirical equations from the literature (a) test site No. 1 (b) test site No. 2.

– Hardin and Drnevich [29]

$$G_0 = \frac{122.2 \cdot (2.97 - e)^2}{1 + e} \cdot \sqrt{Pa \cdot \sigma'_0}$$

(6)

$$G_0 = 445 \cdot \frac{(4.4 - e)^2}{1 + e} \cdot (\sigma'_0)^{0.5}$$

(7)

– Kokusho et al. [35]

$$G_0 = 90 \cdot \frac{(7.32 - e)^2}{1 + e} \cdot (\sigma'_0)^{0.6}$$

(8)

**Table 5**  
Summary of regression and error analysis – test site No. 1 and No. 2.

No.	Expressions	Determination coefficient $R^2$	Standard deviation $SD$ MPa	Mean deviation $MD$ MPa	Mean relative error $MRE$ %	Maximum relative error $MRD$ %	Spread of $\Delta G_{0 \text{ avg}}$ MPa
Test site No. 1							
4	The Authors' equation	0.86	40.4	34.6	13.5	60.0	4
6	Hardin and Drnevich [9]	–	23.7	19.9	–23.6	45.0	–33
7	Marcuson and Wahls [36]	–	21.1	17.7	–29.2	29.2	–40
8	Kokusho et al. [35]	–	0.3	0.2	–99.2	98.7	–103
9	Hardin and Black [5]	–	63.6	53.3	111.5	288.1	87
Test site No. 2							
5	The Authors' equation	0.99	31.1	24.1	–1.1	5.0	1
6	Hardin and Drnevich [9]	–	13.5	10.8	–15.9	15.6	16
7	Marcuson and Wahls [36]	–	12.0	9.6	–25.0	3.1	23
8	Kokusho et al. [35]	–	0.2	0.1	–99.2	–99.0	75
10	Hardin [34]	–	36.7	29.4	128.7	214.5	–86

– Hardin and Black [5]

$$G_0 = \frac{3270 \cdot (2.973 - e)^2}{1 + e} \cdot (\sigma'_m)^{0.5} \quad (9)$$

– Hardin [34]

$$G_0 = \frac{625 \cdot OCR^k}{0.3 + 0.7e^2} \cdot \sqrt{Pa \cdot p'} \quad (10)$$

where  $p' = \sigma'_m = \sigma'_o$  means effective stress,  $Pa$  is atmospheric pressure, equal to 98 kPa, and  $k$  is parameter depend on plasticity index as follows:  $PI=1, 20, 40, 60, 80, 100$  and then respectively  $k=0, 0.18, 0.31, 0.41, 0.48, 0.5$ . Eqs. (6)–(8) describe satisfactory the stiffness of cohesive soils, especially clayey soils (Eqs. (7) and (8)), whereas Eq. (9) is appropriate for normally consolidated cohesive soils and Eq. (10) for overconsolidated cohesive soils.

In Fig. 8a the experimental values of  $G_0$  (test site No. 1) are plotted against the fitting curves predicted by Eqs. (4), (6)–(9), when in Fig. 8b,  $G_0$  from test site No. 2 and Eqs. (5), (6)–(8) and (10) are shown. It is noticeable that the test data of Polish clayey soils in most cases are located outside of the literature curves. The calculated values of  $G_0$  for low stresses only, i.e. up to around 100kPa, may agree to expressions (6) and (7). With increasing mean effective stress, an unsatisfactory behaviour of the Polish Quaternary cohesive soils by the literature formulas is reported here.

It is worth emphasizing that both equations derived by the authors (Eqs. 4 and 5) are characterized by a high value (greater than 0.8) of the determination coefficient  $R^2$  (Table 5). In Table 5, apart from  $R^2$  values, the basic fitting parameters for all studied curves, these ones defined by the authors and the literature curves, are summarized. Using the previous studied in the literature  $G_0$  relationships, the significant differences between the experimental and the calculated values of the low-amplitude shear modulus are observed, spread of  $\Delta G_{0 \text{ avg}}$  ( $\Delta G_{0 \text{ avg}} = G_{0 \text{ avg experimental}} - G_{0 \text{ avg calculated}}$ ) is in the range of –33 to –103 MPa for test site No. 1 and 16 to –86 MPa for test site No. 2. Regarding e.g. the mean relative errors  $MRE$ , the literature curves have the corresponding  $MRE$  values superior to 20% (test site No. 1) or 15% (test site No. 2). The mathematical expressions given in Eqs. (4) and (5) allow to obtain a significantly smaller dispersion of the results, approx. from 1 to 4 MPa, with  $MRE$  equals to 13.5% (test site No. 1) or –1.1% (test site No. 2).

Based on Fig. 8 and Table 5, it can be observed that the authors' expressions fit the tests results perfectly. Obviously, the authors are

aware that their proposed functions require further verification by performing more research on various cohesive soils. The authors remark, however, that their functions are only valid within the cohesive soils studied.

## 6. Final remarks

In the presented study, dynamic properties of normally consolidated and lightly overconsolidated cohesive soils were investigated using the resonant column method. Various types of clayey soils from two different test sites in the Warsaw area were selected. For each type of specimen, wide ranges of the mean effective stress values, void ratios and plasticity index values were considered. The resonant column tests were performed on each specimen. The authors attempted to create an empirical expression describing the soil deformation characteristics in the range of small strains. The main findings achieved in this study are summarized below as follows:

- (1) As anticipated, the mean effective stress  $p'$  had a visible influence on the tested soil stiffness. There was no clear trend observed for the significant effect of other two analysed parameters, i.e. void ratio  $e$  and plasticity index  $PI$ , on the low-amplitude shear modulus  $G_0$  of the Polish Quaternary cohesive soils.
- (2) On the basis of the laboratory tests, some possible correlations between the low-amplitude shear modulus and the stress state were found: Eqs. (4) and (5). Experimental results show nonlinear  $G_0$  versus  $p'$  behaviour that is very well described by a power-law dependence. The values of the coefficient of determination for Eqs. (4) and (5) are greater than 0.8 which suggest that the proposed regression lines approximate very well the real data. The suggested equations are helpful in estimating the shear modulus at small strains without the knowledge of the shear wave velocity, but solely with information about the stress level.
- (3) Using commonly known empirical equations, in their pure form, it is not possible to reliably calculate the low-amplitude shear modulus for the Polish Quaternary cohesive soils. A comparison of the tests data with the equations from the literature resulted in the consequences of the large spread of  $G_0$  values as well as high values of errors.
- (4) The proposed formulas are still preliminary and need verification by being applied at different clayey soils sites. Moreover, the values of the soil stiffness obtained in laboratory and those received from *in situ* seismic tests should be compared. Then, the suggested formulas could be examined by different laboratory and field techniques.

## References

- [1] Lai CG, Pallara O, Lo Presti DCF, Turco E. Low-strain stiffness and material damping ratio coupling in soils. In: Shibuya, Kuwano (eds); *Advanced Laboratory Stress-Strain Testing of Geomaterials*, Tatsuoaka; 2001. p. 265–74.
- [2] Ishimoto M, Iida K. Determination of elastic constants of soils by means of vibration methods, 15. Japan: *Bulletin, Earthquake Research Institute, BUERA*, Tokyo University; 1937. p. 67–85.
- [3] JR Jr Hall, FE Jr Richart. Discussion of elastic wave energy in granular soils. *J Soil Mech Found Div ASCE* 1963;89(SM6):27–56.
- [4] Drnevich VP, Hall JR, Jr FE Richart. Effects of amplitude of vibration on the shear modulus of sand. In: *Proceedings of the international symposium on wave propagation and dynamic properties of earth materials albuquerque*. New Mexico University of New Mexico Press; 1967.
- [5] Hardin BO, Black WL. Vibration modulus of normally consolidated clays. *J Soil Mech Found Div ASCE* 1968;92(SM2):353–69.
- [6] Drnevich VP. Resonant-column problems and solutions. *Dynamic Geotechnical Testing*, ASTM STP 654, ASTM International West Conshohocken PA; 1978. p. 384–98.
- [7] Rayhani MHT, El-Naggar MH. Dynamic properties of soft clay and loose sand from seismic centrifuge tests. *Geotech Geol Eng* 2008;26:593–602.
- [8] Senetakis K, Anastasiadis A, Ptilakis K, Coop MR. The dynamics of a pumice granular soil in dry state under isotropic resonant column testing. *Soil Dyn Earthq Eng* 2013;45:70–9.
- [9] Hardin BO, Drnevich VP. Shear modulus and damping in soils: design equations and curves. *J Soil Mech Found Div ASCE* 1972;98(7):667–92.
- [10] Nie Y, Laun M, Tang X. Study on hollow cylinder torsional shear of dynamic properties of two soils. *Electron J Geotech Eng* 2008;13:1–11.
- [11] Kalinski ME, Thummaluru MSR. A new free-free resonant column device for measurement of  $G_{max}$  and  $D_{min}$  at higher confining stresses. *Geotech Test J ASTM* 2005;28(2):180–7.
- [12] Yang J, Yan XR. Site response to multidirectional earthquake loading a practical procedure. *Soil Dyn Earthq Eng* 2009;29:710–21.
- [13] Schneider JA, Hoyos LJr, Mayne PW, Macari EJ, Rix GJ. Field and laboratory measurements of dynamic shear modulus of Piedmont residual soils. *Behavioural Characteristics of Residual Soils GSP 92 ASCE* Reston VA; 1999. p. 12–25.
- [14] ASTM Standard D4015-92. Test methods for modulus and damping of soils by the resonant-column method. *Annual Book of ASTM Standards*, 4.08. Conshohocken PA: ASTM International West; 2003. p. 473–94.
- [15] Sas W, Gabryś K. Laboratory measurement of shear stiffness in resonant column apparatus. *ACTA Sci Pol Ser Archit* 2012;11(4):29–39.
- [16] Cascante G, Santamarina JC. Low-Strain Measurements Using Random Noise Excitation. *Geotech Test J* 1997;20(1):29–39.
- [17] Cascante G, Santamarina SK, Yassin N. Flexural excitation in a standard torsional-resonant column. *Can Geotech J* 1998;35(3):478–90.
- [18] Khan ZH, Cascante G, El-Naggar MH. Evaluation of the first mode of vibration and base fixidity in resonant-column testing. *Geotech Test J ASTM* 2007;31(1):65–75.
- [19] PN-EN ISO 14688-1. *Badania geotechniczne. Oznaczanie i klasyfikowanie gruntów. Część I: Oznaczanie i opis* [In Polish]. Eurocode 7 – Geotechnical design – Part 1 General rules; 2006.
- [20] PIG 2012. *Raport z badań kontrolnych budowanych nasypów drogowych na Południowej Obwodnicy Warszawy S-2 na odcinku od węzła “Konotopa” do węzła “Lotnisko”*. Warszawa, 20 czerwiec 2012 [In Polish], Report from control tests of road embankments built on the Southern Warsaw Bypass S2 section from junction Konotopa to junction Airport. Warsaw, June 20th; 2012.
- [21] Sas W, Gabryś K, Szymański A. *Analiza sztywności gruntów spoistych przy wykorzystaniu kolumny rezonansowej* [In Polish]. Analysis of stiffness of cohesive soils with the use of resonant column. *Inżynieria Morska i Geotech* 2012;4/2012:370–6.
- [22] Skempton AW. The pore-pressure coefficients A and B. *Géotechnique* 1954;4(4):143–7.
- [23] Flores-Guzmán M, Ovando-Shelley E, Valle-Molina C. Small-strain dynamic characterization of clayey soil from the Tecoco Lake, Mexico. *Soil Dyn Earthq Eng* 2014;63:1–7.
- [24] Amir-Faryar B, Aggour MS. Effect of fibre inclusion on dynamic properties of clay. *Geomech Geoengin* 2016;11(2):104–13.
- [25] Markowska-Lech K, Lech M, Bajda M, Szymański A. Small strain stiffness in overconsolidated Pliocene clays. *Annals of Warsaw University of Life Sciences – SGGW, Land Reclamation*. vol. 45(2); 2013. p. 169–81.
- [26] Vucetic M. Cyclic threshold shear strains in soils. *J Geotech Eng* 1994;120(12):2208–28.
- [27] Lombardi D, Bhattacharya S, Muir Wood D. Dynamic soil-structure interaction of monopole supported wind turbines in cohesive soil. *Soil Dyn Earthq Eng* 2013;49:165–80.
- [28] Cai Y, Dong Q, Wang J, Gu C, Xu C. Measurement of small strain shear modulus of clean and natural sands in saturated condition using bender element test. *Soil Dyn Earthq Eng* 2015;76:100–10.
- [29] Stokoe KH II, Darendeli MB, Andrus RD, Brown LT. Dynamic soil properties: laboratory, field and correlation studies, theme lecture. In: *Proceedings of the second international conference earthquake geotechnical engineering*, Vol. 3, Lisbon, Portugal, June; 1999. p. 811–45.
- [30] Wichtmann T, Navarrete Hernández MA, Triantafyllidis T. On the influence of a non-cohesive fines content on small strain stiffness, modulus degradation and damping of quartz sand. *Soil Dyn Earthq Eng* 2015;69:103–14.
- [31] Pineda JA, Colmenares JE, Hoyos LR. Effect of fabric and weathering intensity on dynamic properties of residual and saprolitic soils via resonant column testing. *Geotech Test J* 2014;37(5):800–16.
- [32] Dobry R, Vucetic M. State-of-the-art report: dynamic properties and response of soft clay deposits. In: *Proceedings of the international symposium on geotechnical engineering of soft soils 1987*; 2. p. 51–87.
- [33] Dobry R, Vucetic M. Effect of soil plasticity on cyclic response. *J Geotech Eng* 1991;117(1):89–107.
- [34] Hardin BO. The nature of stress-strain behaviour for soils. In: *Proceedings of the ASCE geotechnical engineering division specialty conference on earthquake engineering and soil dynamics*. vol. 1; 1978. p. 3–90.
- [35] Kokusho T, Yoshida Y, Esashi Y. Dynamic properties of soft clay for wide strain range. *Soil Found* 1982;22(4):1–18.
- [36] Marcuson WF, Wahls HE. Time effects on dynamic shear modulus of clays. *J Soil Mech Found Div ASCE* 1972;98(12):1359–73.